JOURNAL OF GEOPHYSICAL RESEARCH, VOL. 94, NO. B5, PAGES 5560–5570, MAY 10, 1989

Present-Day Motion Along the Owen Fracture Zone and Dalrymple Trough in the Arabian Sea

RICHARD G. GORDON AND CHARLES DEMETS[1]

Department of Geological Sciences, Northwestern University, Evanston, Illinois

All plate motion data available for describing the present-day motion between the Arabian and Indian plates are analyzed to understand the present-day tectonic role of the presumed plate boundary: the Owen fracture zone and Dalrymple trough in the northern Arabian Sea. All prior plate motion models are shown to be inconsistent with some of the data along the presumed boundary. In particular, published global plate motion models predict some convergence across the Owen fracture zone and Dalrymple trough. Convergence along the Owen fracture zone is contradicted by earthquake focal mechanisms, which show right-lateral strike slip. Convergence along the Dalrymple trough is contradicted by observed normal faulting in the trough, and by normal and strike-slip focal mechanisms for earthquakes occurring along or near the trough. The sense and rate of motion is further constrained by spreading rates along the Sheba Ridge (northwest of the Owen fracture zone) and along the Carlsberg Ridge (southeast of the Owen fracture zone). To estimate the present-day motion, we determine 43 3-m.y.-average spreading rates from Sheba Ridge, Carlsberg Ridge, and Central Indian Ridge magnetic profiles and have combined them with eight transform azimuths and 15 earthquake slip vectors along these ridges and the Arabia-India boundary. We determine an Arabia-India Euler vector that predicts 2 mm/yr of right-lateral strike-slip motion along the Owen fracture zone, with a 95% confidence interval of 0–7 mm/yr, which excludes the faster rates of slips predicted by several prior models. The direction of motion is 35°–50° counterclockwise from that predicted by published global plate motion models. If we omit the data along the Arabia-India boundary, the motion differs insignificantly from zero, suggesting that magnetic profiles from the Carlsberg and Sheba ridges give spreading rates too imprecise to detect the slow Arabia-India motion. If the Owen fracture zone and Dalrymple trough are regarded as a plate boundary, it is the slowest slipping plate boundary known on Earth, with motion about 100 times slower than the fastest slipping faults along the East Pacific Rise.

INTRODUCTION

A tenet of the transform fault model is that deformation along oceanic fracture zones is confined to the segment between offset spreading centers, which is consistent with nearly all observed oceanic seismicity [*Sykes*, 1967]. A notable exception is the Owen fracture zone, which is seismically active northeast of where it offsets the Sheba and Carlsberg ridges (Figure 1) [*Matthews*, 1966; *Sykes*, 1968; *Quittmeyer and Kafka*, 1984]. Hereinafter we will refer to the part of the fracture zone offsetting the Sheba and Carlsberg ridges as the Owen transform fault and refer to the part northeast of the Sheba Ridge as the Owen fracture zone (Figure 1). *Matthews* [1966] was the first to map the extent of the Owen fracture zone and transform fault and to note they are seismically active. From the right-lateral offset between the Carlsberg Ridge and eastern Sheba Ridge he proposed that right-lateral motion now occurs along both the Owen fracture zone and the Owen transform fault. *Wilson* [1965], in his seminal paper on transform faults, proposed that slip along both is not right-lateral, but left-lateral. Earthquake focal mechanisms show that neither model is correct. The sense of slip along the Owen transform fault is left-lateral, while the slip along the Owen fracture zone is right-lateral [*Sykes*, 1968; *Quittmeyer and Kafka*, 1984].

Later plate motion models [*McKenzie and Sclater*, 1971; *Chase*, 1972, 1978; *Minster et al.*, 1974; *Minster and Jordan*, 1978] assume left-lateral slip along the Owen transform fault and right-lateral slip along the Owen fracture zone. Although these models agree with the observed sense of slip, some models [e.g., *Chase*, 1978; *Minster and Jordan*, 1978] predict directions of plate motion significantly different from the observed strike of the Owen fracture zone and from the orientation of slip vectors from earthquakes along it (Figures 5 and 7). The rate of motion predicted along the Owen fracture zone by different prior models varies considerably, from 10 to 16 mm/yr at 18.0°N, 60.2°E.

Other studies, which focused on the spreading rates determined from marine magnetic anomalies along the Carlsberg and eastern Sheba ridges, concluded that little or no motion occurs along the Owen fracture zone. *Laughton et al.* [1970] and *Cochran* [1981] have suggested that motion along the Owen fracture zone cannot exceed a few millimeters per year, and *Wiens et al.* [1985] have proposed that the motion is negligible. Because the entire Owen fracture zone does not follow a small circle, as expected if it is a transform fault, *Whitmarsh* [1979] argued that the Owen fracture zone is inactive.

[1]Now at Naval Research Laboratory, Washington, D.C.

Paper number 88JB03855.
0148-0227/89/88JB-03855$05.00

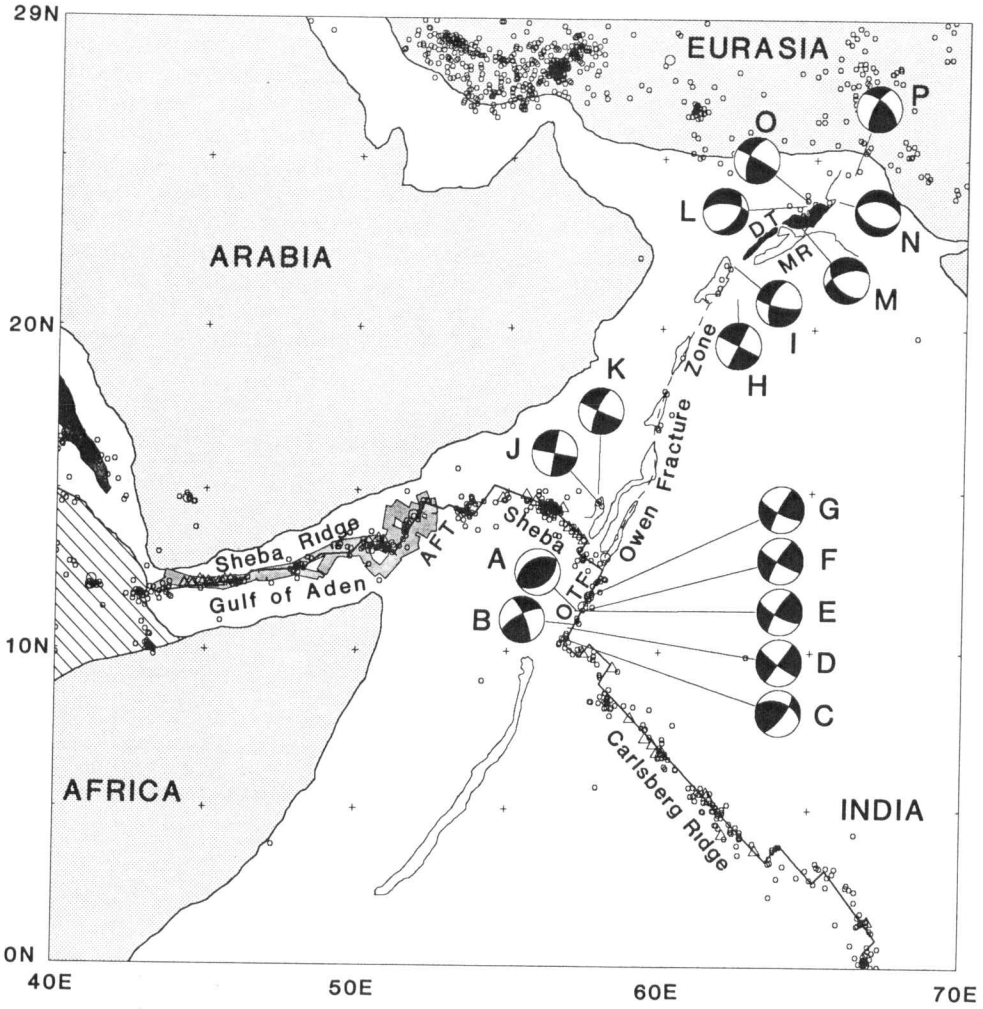

Fig. 1. Location map, major bathymetric features, shallow seismicity, and all available focal mechanisms along and near the Owen fracture zone and Dalrymple trough. Circles show the locations of earthquakes shallower than 50 km from January 1963 to December 1985. Nearly all the earthquakes had magnitudes less than 5.5, but a few larger earthquakes, with magnitudes between 5.5 and 7.0, are shown by slightly larger circles. Locations of magnetic profiles used to determine the spreading rates listed in Table 1 are marked by small open triangles along the ridges. The extent of GLORIA coverage along the Sheba Ridge is the shaded region in the Gulf of Aden. "DT" labels the Dalrymple trough (shown in solid black), "MR" labels the Murray ridge, "AFT" labels the Alula-Fartak transform fault, and "OTF" labels the Owen transform fault. The CMT epicenter is shown for event H; the International Seismological Centre epicenter, which is along the Owen fracture zone and northwest of the CMT epicenter, is probably more accurate. Shallow areas of the Owen ridge and Murray ridge are outlined. Thin dashed line shows the trace of the Owen fracture zone.

In a recent plate motion model, *Wiens et al.* [1985] proposed that no motion occurs along the Owen fracture zone and that India is divided from Australia by a diffuse plate boundary, which extends from the equatorial Central Indian Ridge to the Ninetyeast Ridge where it continues northward along the ridge into the Andaman trench. *Wiens et al.* [1985] argued that the seismic slip rate in the diffuse plate boundary is ~80 times greater than the seismic slip rate along the Owen fracture zone. An advantage of the model of *Wiens et al.* [1985] is that it does not increase the number of Euler vectors needed to describe plate motions in the Indian Ocean, because one plate boundary is eliminated while one is added. However, their model fails to explain several key observations. First, as shown by *Quittmeyer and Kafka* [1984], and as will be documented further here, several earthquakes show a consistent sense of right-lateral slip along the Owen fracture zone. Second, marine reflection seismic profiles show that the Dalrymple trough, which joins the northern end of the Owen fracture zone and trends more easterly than the fracture zone, is extending through listric normal faulting [*White*, 1984]. Moreover, as we will show later, three normal faulting earthquakes occur within or near the Dalrymple trough. These observations fall into a consistent pattern: extension along the Dalrymple trough is expected if pure right-lateral strike slip occurs along the Owen fracture zone. Therefore models that neglect motion along the Owen fracture zone conflict with some observations.

Here we develop a new quantitative model for motion along the India-Arabia plate boundary (i.e., the Owen fracture zone and Dalrymple trough) by inverting all available plate motion data including spreading rates from magnetic profiles across the Sheba, Carlsberg, and

northern Central Indian ridges, strikes of transform faults, and slip vectors from earthquake focal mechanisms. All spreading rates used here were determined by comparing observed magnetic profiles to synthetic magnetic anomaly profiles we computed. Unlike *Chase* [1978] and *Minster and Jordan* [1978], we follow *Wiens et al.* [1985] in assuming that India and Australia lie on separate plates divided by a diffuse plate boundary extending from the equatorial Central Indian Ridge, through Chagos Bank and Ninetyeast Ridge, to the Sumatra Trench. The Indian plate that we refer to here includes India but not Australia, and should not be confused with the "Indian plate" referred to by many prior workers [e.g., *Chase*, 1978; *Minster and Jordan* 1978], as the latter plate contains both India and Australia. We will refer to this latter hypothetical plate as the Indo-Australian plate.

There are two further differences from some prior work. First, in this paper we incorporate azimuth data along the Arabia-India plate boundary. No data along this boundary were included, for example, by *Minster and Jordan* [1978]. Second, because we assume that the Indian and Australian plates are divided by a boundary that intersects the Central Indian Ridge near the equator, we do not try to fit all data along the Carlsberg Ridge

TABLE 1*a*. Northern Indian Ocean Plate Motion Data: Arabia-India (Owen Fracture Zone and Dalrymple Trough)

Latitude, °N	Longitude, °E	Datum	σ	Model	I	Source
			Fault Azimuths			
18.00	60.20	S23°W	5°	S22°W	0.535	*Mathews* [1966]
21.00	61.80	S30°W	5°	S28°W	0.459	*Mathews* [1966]
			Slip Vectors			
24.58	66.23	S41°W	15°	S37°W	0.270	*Quittmeyer and Kafka* [1984]
23.79	64.73	S28°W	15°	S35°W	0.176	*Quittmeyer and Kafka* [1984]
21.87	62.32	S12°W	15°	S29°W	0.067	*Quittmeyer and Kafka* [1984]
20.91	62.44	S26°W	15°	S28°W	0.055	*Dziewonski et al.* [1986*a*]
14.94	57.96	S23°W	15°	S16°W	0.171	*Dziewonski et al.* [1986*b*]
14.57	58.09	S10°W	15°	S17°W	0.189	*Dziewonski and Woodhouse* [1983]

The standard error assigned to each datum is σ. The datum importance is I, which measures the information content of each datum [*Minster et al.*, 1974].

TABLE 1*b*. Northern Indian Ocean Plate Motion Data: Africa-India (Carlsberg and Northern Central Indian Ridges)

Latitude, °N	Longitude, °E	Datum	σ	Model	I	Ridge Strike	Source
				Spreading Rates			
9.95	57.51	25	3	24.5	0.175	S60°E	NGDC *USS Wilkes*
9.50	58.50	27	4	25.3	0.084	S60°E	*McKenzie and Sclater* [1971]
7.90	59.10	26	4	25.9	0.057	S50°E	*McKenzie and Sclater* [1971]
7.25	59.60	27	3	26.5	0.093	S50°E	NGDC *USS Wilkes*
7.06	59.87	28	3	26.7	0.091	S50°E	NGDC† *Vema* 19-10
6.80	60.00	29*	3	26.9	0.089	S50°E	*McKenzie and Sclater* [1971]
6.84	60.16	25	4	27.0	0.050	S50°E	NGDC† *Vema* 19-10
6.72	60.18	25	3	27.0	0.088	S50°E	NGDC† *Vema* 19-10
5.54	61.66	29	3	28.3	0.088	S50°E	NGDC Indomed 4
5.43	61.70	29	3	28.4	0.088	S50°E	NGDC *Vema* 34 08
5.30	61.80	27	4	28.5	0.050	S50°E	*McKenzie and Sclater* [1971]
4.20	62.20	28	4	29.1	0.055	S50°E	*McKenzie and Sclater* [1971]
4.20	62.20	27*	5	29.1	0.035	S50°E	*McKenzie and Sclater* [1971]
3.70	63.30	29	5	29.9	0.041	S50°E	*McKenzie and Sclater* [1971]
1.47	67.01	33	10	32.2	0.021	S45°E	NGDC *Chain* 100 5
-0.05	67.35	33	10	33.0	0.026	S45°E	NGDC Antipodes 10
-0.10	67.17	32	10	32.9	0.026	S45°E	NGDC *Vema* 34 6
-2.83	67.10	32	5	30.4	0.162	S25°E	NGDC *Conrad* 12 15
				Fault Azimuths			
11.00	57.50	S30°W	5°	S28°W	0.206		*Laughton et al.* [1970]
0.50	67.00	S43°W	10°	S35°W	0.047		*McKenzie and Sclater* [1971]
				Slip vectors			
11.74	57.71	S28°W	15°	S27°W	0.022		A. M. Dziewonski et al. (unpublished data, 1987)
11.28	57.25	S29°W	15°	S28°W	0.023		*Dziewonski et al.* [1987*c*]
11.28	57.49	S29°W	15°	S28°W	0.023		*Dziewonski et al.* [1983*a*]
10.76	57.00	S36°W	15°	S29°W	0.024		*Dziewonski et al.* [1987*a*]
-1.00	67.45	S34°W	15°	S36°W	0.023		*Dziewonski et al.* [1986*a*]
-1.40	67.77	S35°W	15°	S36°W	0.023		*Dziewonski et al.* [1986*a*]
-1.41	67.75	S37°W	15°	S36°W	0.023		*Dziewonski and Woodhouse* [1983]

The datum, model, and σ for spreading rates are in mm/yr.
* Rates determined from aeromagnetic profiles.
† Previously published profiles [*McKenzie and Sclater*, 1971], which we obtained from the NGDC for the present analysis.

TABLE 1c. Northern Indian Ocean Plate Motion Data: Africa-Arabia (Sheba Ridge, Gulf of Aden)

Latitude, °N	Longitude, °E	Datum	σ	Model	I	Ridge Strike	Source
				Spreading Rates			
13.50	57.50	24	4	25.2	0.053	S58°E	*Cochran* [1981]
13.70	57.30	25	4	25.0	0.051	S58°E	*Cochran* [1981]
13.90	57.00	25	4	24.7	0.048	S58°E	*Cochran* [1981]
14.50	56.80	24	3	24.4	0.078	S58°E	*Cochran* [1981]
14.60	56.40	24	3	24.1	0.072	S58°E	*Cochran* [1981]
14.70	55.90	24	3	23.6	0.092	S80°E	*Cochran* [1981]
14.90	55.60	23.5	3	23.8	0.078	S73°E	*Laughton et al.* [1970]
14.80	54.80	23	3	23.3	0.068	S73°E	*Laughton et al.* [1970]
14.41	53.60	24	3	22.6	0.056	S73°E	*Laughton et al.* [1970]
13.20	51.00	19	4	21.5	0.023	S68°E	*Cochran* [1981]
13.40	50.90	21	4	21.3	0.023	S68°E	*Laughton et al.* [1970]
13.50	50.70	21	3	21.2	0.039	S68°E	*Laughton et al.* [1970]
13.40	50.40	21.5	3	21.0	0.038	S70°E	*Tamsett and Girdler* [1982]
12.15	45.85	15	2.5	17.3	0.063	S80°E	*Girdler et al.* [1980]
12.15	45.65	18.5	2.5	17.1	0.065	S80°E	*Girdler et al.* [1980]
12.10	45.55	16	2.5	17.1	0.066	S80°E	*Tamsett and Girdler* [1982]
12.08	45.47	18.5	2.5	17.0	0.067	S80°E	*Girdler et al.* [1980]
12.05	45.25	17.5	2.5	16.9	0.069	S80°E	*Girdler et al.* [1980]
12.05	45.17	16.5	2.5	16.8	0.070	S80°E	*Girdler et al.* [1980]
12.10	45.10	16.5	2.5	16.8	0.071	S80°E	*Girdler et al.* [1980]
12.10	44.92	16.5	2.5	16.6	0.073	S80°E	*Girdler et al.* [1980]
12.15	44.81	16	2.5	16.6	0.075	S80°E	*Girdler et al.* [1980]
12.05	44.59	15.5	2.5	15.7	0.077	S85°E	*Girdler et al.* [1980]
12.08	44.50	15.5	2.5	15.6	0.078	S85°E	*Girdler et al.* [1980]
12.05	44.29	16.5	2.5	15.5	0.081	S85°E	*Girdler et al.* [1980]
				Fault Azimuths			
13.90	51.70	S26°W	5°	S26°W	0.214		R. Searle (personal communication, 1987)
13.30	49.60	S29°W	7°	S28°W	0.105		*Tamsett and Searle* [1987]
13.20	49.40	S28°W	5°	S28°W	0.203		*Tamsett and Searle* [1987]
12.60	48.00	S25°W	5°	S30°W	0.199		*Tamsett and Searle* [1987]
				Slip Vectors			
14.29	51.82	S28°W	15°	S25°W	0.025		PDE (January, 1984)
14.00	51.70	S30°W	15°	S25°W	0.024		*Sykes* [1970]

The datum, model, and σ for spreading rates are in mm/yr.

and entire Central Indian Ridge with a single Euler vector. We believe that the poor agreement of prior models with data along the Owen fracture zone and Carlsberg Ridge is caused, at least in part, by incorrectly assuming that the Indian plate extends far south of the equator.

We find the best estimate of the slip rate along the Owen fracture zone is only 2 mm/yr in a direction 35°–50° counterclockwise from that predicted by the models of *Chase* [1978] and *Minster and Jordan* [1978]. If the Owen fracture zone can properly be considered to be a plate boundary, the best estimate of the rate of motion is remarkably slow, about 100 times slower than the motion along the fastest slipping transform faults along the East Pacific Rise.

THE DATA

Carlsberg Ridge and Owen Transform Fault

Magnetic profiles used to determine rates across the Carlsberg Ridge are from two sources: the National Geophysical Data Center (NGDC) magnetic data archives, and *McKenzie and Sclater* [1971] (Table 1). Along the Carlsberg Ridge, we determined 18 rates: 11 from NGDC data, the remaining 7 from enlarged versions of figures from *McKenzie and Sclater* [1971]. All but one rate in Table 1 were determined from single profiles. The one rate not determined from a single profile was determined from several closely spaced incomplete magnetic profiles shown by *McKenzie and Sclater* [1971] near 9.5°N, 58.5°E. Four of the rates from NGDC data are from unpublished profiles, which were collected in 1977 and 1978, were navigated by satellite, and were observed along nearly ridge-normal tracks (Figure 2). The Carlsberg Ridge data include two aeromagnetic profiles, which have high signal to noise ratios owing to the rapid decay with height of the anomaly caused by three-dimensional structures, such as seamounts, relative to the anomaly from two-dimensional magnetic sources, such as those created by seafloor spreading stripes [*McKenzie and Sclater*, 1971]. The aeromagnetic profiles give us some confidence that our correlations are not systematically in error.

The direction of India-Africa motion was determined from the trend of the Owen and a near-equatorial transform fault and from seven slip vectors, four from Owen transform fault earthquakes (D–G in Figure 1 and Table 2) and three from near-equatorial earthquakes (Table 1). We excluded three centroid-moment tensor solutions for events on the Owen transform fault (Figure 1, Table 2). The epicenter of event A (a pure thrust

mechanism with a surface wave magnitude of ~6.1) estimated by *Dziewonski et al.* [1987*a*] differs from the International Seismological Centre epicenter by 100 km, suggesting it is located incorrectly. Event B, located on the Owen transform and modeled by *Dziewonski et al.* [1987b], had a surface wave magnitude less than 4.5, which may be too small to give a reliable slip vector. We omitted event C because it occurred near the ridge-transform intersection. The remaining events (D–G) located along the Owen transform fault are strike-slip mechanisms with left-lateral slip along a nodal plane parallel or subparallel to the strike of the transform fault, as expected.

Sheba Ridge

Bathymetry and magnetic anomalies are well mapped in the Gulf of Aden. We determined spreading rates in the eastern Gulf of Aden by comparing enlargements of magnetic profiles shown in the papers by *Cochran* [1981] and *Laughton et al.* [1970] to synthetic magnetic anomaly profiles that we computed. Some of these observed and synthetic profiles are shown in Figures 3a and 3b. A high-density surface-ship study of Sheba Ridge magnetics in the western Gulf of Aden [*Girdler et al.*, 1980] establishes the spreading rate there to within 2 mm/yr (Figure 3b). To avoid bias caused by rift propagation [*Courtillot et al.*, 1980], no magnetic profiles west of 44.25°E were used.

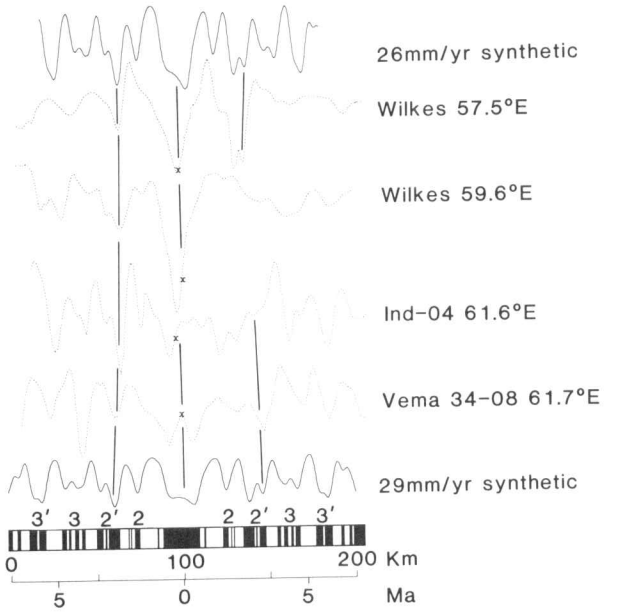

Fig. 2. All post-1971 Carlsberg Ridge magnetic profiles west of 65°E available from the NGDC. From top to bottom the profiles (dashed lines) are from the following cruises: *USS Wilkes* (1978), *USS Wilkes* (1978), Indomed Leg 4 (1978), and *Vema* 34 (1977). The top profile is projected onto N30°E; the other three are projected onto N40°E. The bathymetrically defined axis of the ridge is marked with a cross. When computing the synthetic magnetic anomaly profiles (solid curves), we assumed the depth to the magnetic layer to be 3 km and the transition width to be 1 km. Vertical lines connect either the ridge axis or anomaly 2′ on a profile to the same feature on an adjacent profile. The rough bathymetry along these tracks is typical of slow spreading rates, degrades the quality of the magnetic anomalies, and makes it hard to identify fracture zones. Anomaly 2′ cannot be unambiguously identified on both sides of the ridge axis from any single profile shown. Instead, anomaly 2′ is identified from its location relative to the ridge axis, the identification of adjacent anomalies and, most importantly, comparison to synthetic magnetic anomalies computed for many alternative spreading rates. The existence and spacing of anomalies 3 and 3′ supports our identification of anomaly 2′ in the lower two profiles. All other Carlsberg Ridge profiles west of 65°E that we use in this paper are shown by *McKenzie and Sclater* [1971] and typically are of a quality similar to the profiles shown here. These newer profiles are best fit by spreading rates similar to those estimated by *McKenzie and Sclater* [1971] from the older profiles.

We determined azimuths from four transform faults along the Sheba Ridge from the orientations of lineaments on line drawings constructed from GLORIA sonographs by D. Tamsett and R. Searle (personal communication, 1987). The present slip direction along the Alula-Fartak transform fault, the longest transform offsetting the Sheba Ridge, is uncertain. Tamsett and Searle have identified a straight, 50-km-long lineament oriented ~N30°E that may be the principal transform displacement zone; however, a histogram of transform lineaments has a peak at N22°–24°E, which Tamsett and Searle suggest could also represent the present slip direction. Given these ambiguities, we adopted a N26±5°E trend for the Alula-Fartak transform. From Tamsett and Searle's interpretations of GLORIA sonographs we also estimated the trends of three shorter offset (35, 40, and 45 km) transforms located west of the Alula-Fartak transform fault. No unambiguous principal transform displacement zones can be recognized in these transform faults. We estimated trends of N25°–29°E, which are 2°–10° counterclockwise from trends used in prior studies.

Two slip vectors from the Gulf of Aden, both located on the Alula-Fartak transform, were used. Their directions agree with the strike of the Alula-Fartak determined from the GLORIA survey.

Owen Fracture Zone and Dalrymple Trough

Two slip vectors (H and I) and two trends measured from the bathymetry (Figure 1) were used to estimate the direction of plate motion along the Owen fracture zone. Additional data used to estimate the Arabia-India direction of motion were slip vectors from earthquakes (J and K) west of the southern Owen fracture zone, a slip vector from a strike-slip earthquake (O) within or near the northwest Dalrymple trough (Figure 1), and a slip vector from a strike-slip earthquake (P) between the Dalrymple trough and the Pakistan coast (Figure 1). These slip vectors were selected from three mechanisms determined by *Quittmeyer and Kafka* [1984] and six centroid-moment tensor solutions from previously unstudied events along the probable Arabia-India plate boundary. The March 19, 1987, May 29, 1977, and May 24, 1978, earthquakes (L, M, and N in Figure 1 and Table 2), located within or near the Dalrymple trough, each show a large component of normal faulting, as is expected if motion along the northern Owen fracture zone is purely strike slip. Slip vectors from these normal faulting earthquakes are not used in our inversion but are compared to the predicted slip direction below. The six dominantly strike-slip mechanisms (H–K, O, and P) are consistent with right-

TABLE 2. Focal Mechanism Parameters: Owen Transform and Fracture Zone and Dalrymple Trough

Event	Date	Latitude, °N	Longitude, °E	ψ, deg	θ, deg	λ, deg	Horizontal Slip, deg	Source
A	July 7, 1986	11.29	57.33*	242	42	98	—	*Dziewonski et al.* [1987*a*]
B	Sept. 29, 1986	10.87	57.20	242	72	167	—	*Dziewonski et al.* [1987*a*]
C	July 29, 1983	10.41	56.88	37	71	44	N20E	*Dziewonski et al.* [1984]
D	Sept. 17, 1986	10.76	57.00	36	89	-9	N36E	*Dziewonski et al.* [1987*b*]
E	May 30, 1978	11.28	57.25	212	79	17	N29E	*Dziewonski et al.* [1987*c*]
F	April 8, 1983	11.28	57.49	211	80	9	N29E	*Dziewonski et al.* [1983]
G	April 20, 1980	11.74	57.71	208	83	15	N28E	Dziewonski et al. (unpublished data, 1987)
H	April 7, 1985	20.91	62.44†	206	90	180	S26W	*Dziewonski et al.* [1986*a*]
I	March 30, 1966	21.87	62.32	200	60	195	S12W	*Quittmeyer and Kafka* [1984]
J	Dec. 5, 1981	14.57	58.09	190	90	180	S10W	*Dziewonski and Woodhouse* [1983]
K	Dec. 14, 1985	14.94	57.96	204	76	-177	S23W	*Dziewonski et al.* [1986*b*]
L	March 19, 1987	23.67	64.66	272	62	-54	S08E	A. M. Dziewonski et al. (unpublished data, 1987)
M	May 29,1977	23.07	64.47	252	61	-133	S24W	*Dziewonski et al.* [1987*b*]
N	May 24, 1978	23.80	65.72	277	50	-98	S13W	*Dziewonski et al.* [1987*c*]
O	Nov. 9, 1968	23.79	64.73	205	60	355	S28W	*Quittmeyer and Kafka* [1984]
P	April 4, 1968	24.58	66.23	210	70	330	S41W	*Quittmeyer and Kafka* [1984]

* The International Seismological Centre (ISC) epicenter is 10.40°N, 57.30°E. † ISC location is 21.20°N, 61.93°E. Strike (ψ) is measured clockwise from north; dip (θ) is rotated clockwise from the strike; slip (λ) is counterclockwise from the strike and is in the fault plane.

lateral strike slip parallel to the Owen fracture zone. For each earthquake we took the fault plane to be the nodal plane closest in strike to the Owen fracture zone.

The December 5, 1981, and December 14, 1985, earthquakes (J and K in Figure 1 and Table 2) are near the southern Owen fracture zone. Interestingly, however, they are located not along the bathymetrically defined trace of the Owen fracture zone (dashed line in Figure 1), but lie 85 and 100 km northwest of it, at the edge of a region of northeast striking lineaments (Figure 1). As we will show later in Figure 5, the strike of this seismically quiet segment of the Owen fracture zone is about 10° clockwise from the predicted direction of plate motion, consistent with it being inactive or only part of a wider plate boundary zone. Although the Owen fracture zone south of 17°N appears seismically inactive since 1963, *Gutenberg and Richter* [1954] report two or three events near this southern segment (Figure 7). The accuracy of these older locations is not as good, and it is unclear whether they occurred along the Owen fracture zone.

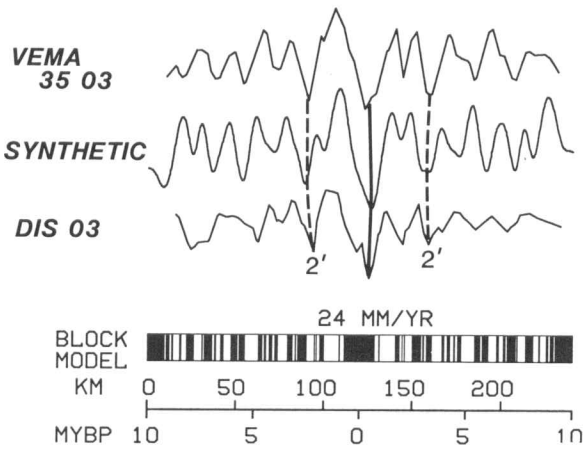

Fig. 3*a*. Magnetic anomaly profiles typical of the best data available from the eastern Sheba Ridge [*Laughton et al.*, 1970; *Cochran*, 1981]. Upper profile is *Vema* 35-03; middle profile is a synthetic magnetic anomaly profile computed for 24 mm/yr; lower profile is *Discovery* 03. All profiles are shown here projected onto N32°E. In our analysis the best fit rates are corrected to what they would have been if collected along tracks orthogonal to the Sheba Ridge, which strikes about N60°W in this region.

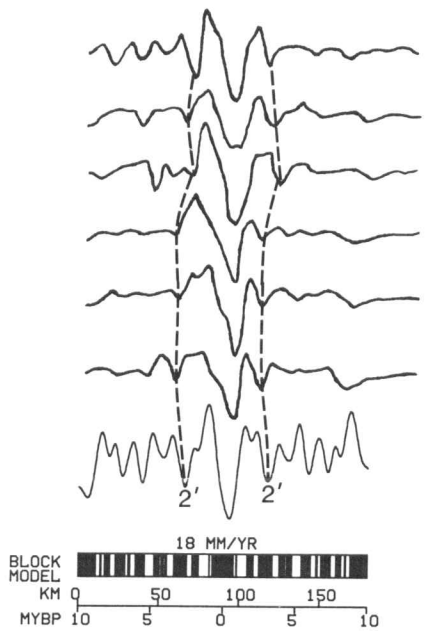

Fig. 3b. Magnetic anomaly profiles typical of the better data available from the western Gulf of Aden [*Girdler et al.*, 1980]. These profiles are each shown along track (N32°E). In our analysis the best fit rates are reduced to what they would have been if collected along tracks orthogonal to the Sheba Ridge, which strikes N80-85°W in this region.

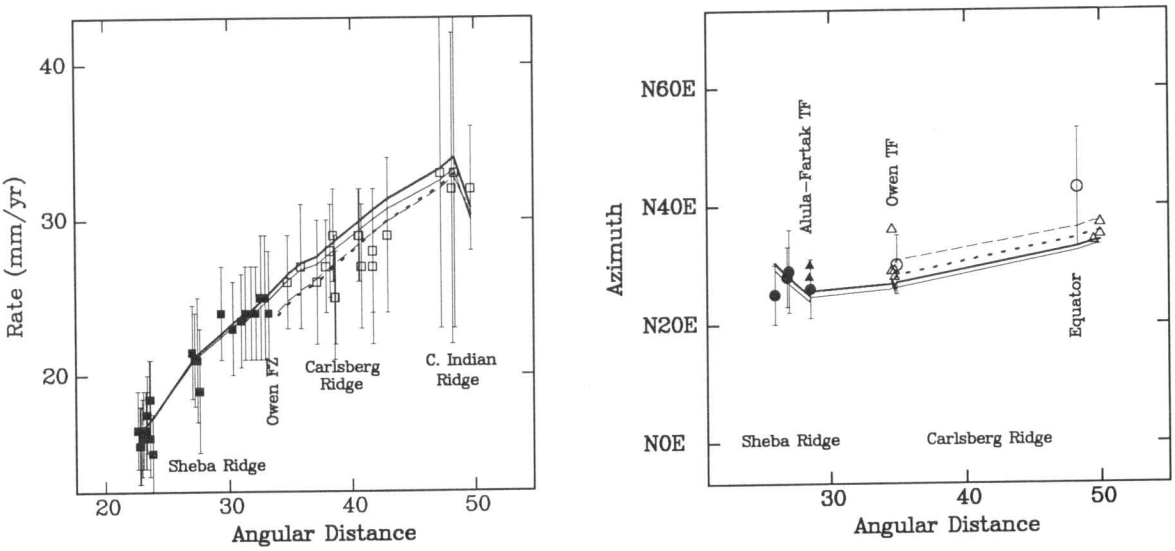

Fig. 4. Plate motion data observed along the Sheba, Carlsberg, and equatorial Central Indian ridges are compared to rates and azimuths calculated from different plate motion models. Squares show seafloor spreading rates determined from surface and aeromagnetic profiles, circles show observed transform fault azimuths, and triangles show observed slip vector azimuths. Symbols are solid if along the Sheba Ridge, open otherwise. The bold solid curve in each panel was calculated from the Arabia-Africa Euler vector determined from simultaneously inverting data along all three plate boundaries. This three-plate model is similar to the Arabia-Africa Euler vector determined from data only along the Sheba Ridge (thin solid curve). Similarly, the India-Africa three-plate Euler vector (short-dashed curve) gives rates and azimuths similar to those calculated from the India-Africa Euler vector determined from data only along the Carlsberg and equatorial Central Indian ridges (long-dashed curve). The tendency for rates observed along the Carlsberg Ridge to be a few mm/yr less than predicted by the curve fit to the Sheba Ridge data suggests that right-lateral slip of about 2 mm/yr occurs along the Owen fracture zone.

COMPARISON OF SPREADING RATES ALONG THE SHEBA AND CARLSBERG RIDGES

We first tested for motion along the Owen fracture zone using spreading rates, transform azimuths, and slip vectors along the Sheba and Carlsberg ridges, but using no data along the Owen fracture zone and Dalrymple trough. We used the following reasoning: If there is no motion along the Owen fracture zone, then an Arabia-Africa Euler vector determined from data only along the Sheba Ridge should predict rates along the Carlsberg Ridge that agree with observed rates. Instead, if significant right-lateral slip is occurring along the Owen fracture zone, then the observed Carlsberg Ridge rates should be systematically less than predicted. Conversely, if significant left-lateral slip were occurring, the observed rates would be systematically greater than predicted. The Arabia-Africa Euler vector was determined using methods described in a prior paper [*DeMets et al.*, 1988].

The results of this test show that the agreement between predicted and observed rates is good but not perfect (see the thin solid curve in Figure 4). The good agreement shows that any motion along the Owen fracture zone must be significantly smaller than the 10–16 mm/yr calculated from the plate motion models of *McKenzie and Sclater* [1971], *Chase* [1978], and *Minster and Jordan* [1978]. An F ratio test for additional plate boundaries [*Stein and Gordon*, 1984] suggest that any motion along the boundary is insignificant, a result consistent with the interpretations of *Laughton et al.* [1970], *Cochran* [1981], and *Wiens et al.* [1985]. On close inspection, however, it can be seen that the observed rates tend to be a few mm/yr slower than predicted, consistent with a few mm/yr right-lateral slip along the Owen fracture zone.

PLATE MOTION MODEL

The next step in our analysis was to add the azimuthal data along the Owen fracture zone and Dalrymple trough to the data along the ridges to test whether a model consistent with all the observations could be determined and, if so, find the best-fitting model and its uncertainties. We assumed that the plate motion data reflected motion between three plates: Arabia, Africa, and India. The Sheba Ridge divides the Arabian from the African plate; the Owen fracture zone and Dalrymple trough divide the Arabian from the Indian plate; the Carlsberg and northernmost Central Indian ridges divide the Indian from the African plate (Figure 1). Using an approach like that of *Chase* [1978] and *Minster and Jordan* [1978], we force our model to be consistent with plate circuit closure. With this approach, a model found to be consistent with all the data will also be consistent with plate circuit closure and rigid plate tectonics. An F ratio test for plate circuit closure [*Gordon et al.*, 1987] gives F=2.3 ($F_{.01}$=5.0 for 2 versus 58 degrees of freedom), suggesting that the data are consistent with plate circuit closure.

Figures 4 and 5 show that a plate motion model consistent with the data can be found (Table 3). The direction of motion along the Owen fracture zone is determined mainly by the Arabia-India azimuthal data, whereas the rate of motion reflects the small difference in

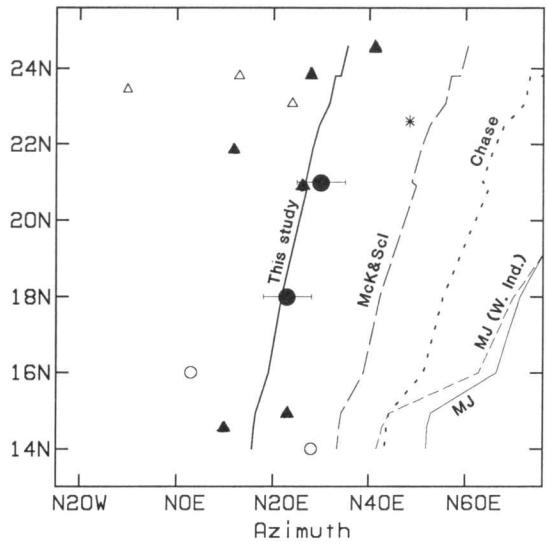

Fig. 5. Fit of the Arabia-India closure-enforced Euler vector to azimuths along the Arabia-India plate boundary. Circles are observed strikes of submarine features. The two solid circles are measured strikes along the northern Owen fracture zone and were used in the inversion. The open circles at 14°N and 16°N are strikes along the southern, seismically quiet segment of the fracture zone and are shown only for comparison. Triangles are slip vectors from earthquakes along the Owen fracture zone and Murray ridge. Solid triangles are strike-slip events, which were used in the inversion, whereas open triangles are normal-faulting events, which are shown only for comparison. The asterisk shows the strike of the Dalrymple trough, which was not used in the inversion; the difference between the model and the observed strike of the Dalrymple trough shows that the model predicts a component of extension across the trough, in agreement with interpretations of marine seismic reflection profiles [*White*, 1984]. Older plate motion models (thin solid and various dashed curves) predict azimuths 15°–60° clockwise of observed azimuths, whereas the model presented here (bold solid curve) agrees well with the observations.

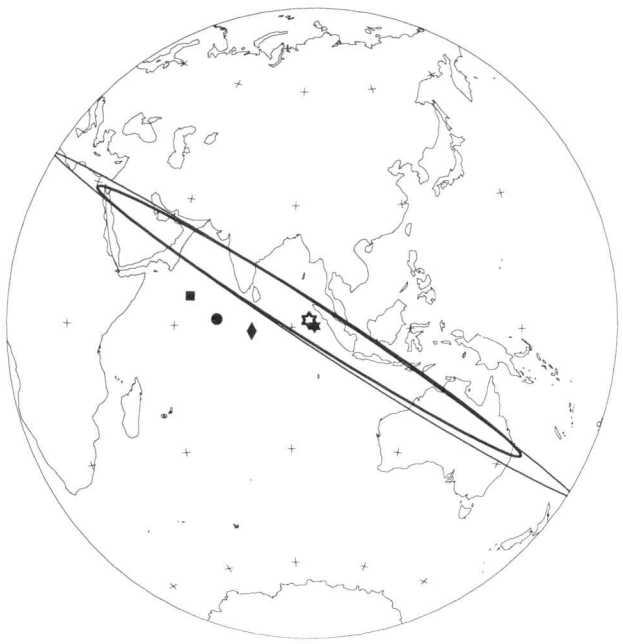

Fig. 6. Current India-Arabia Euler poles. The 95% confidence limit on the three-plate Euler pole (open star) is shown with a thicker curve than the limit on the best-fitting Euler pole (solid star). The Euler poles from prior studies lie outside the confidence limits of the new poles. The square is the pole of *Minster and Jordan* [1978], the circle is the pole of *Chase* [1978], and the diamond is the pole of *McKenzie and Sclater* [1971].

spreading rates between the Carlsberg and Sheba ridges. A best-fitting Euler pole and confidence limits derived from the Arabia-India azimuths agrees with the Euler vector determined here from the three-plate Arabia-India-Africa circuit and excludes the Euler poles of prior models (Figure 6). That a model can be found that is consistent with the slip vectors from earthquakes separated by as much as 1400 km along the Owen fracture zone and Dalrymple trough attests to the usefulness of treating the fracture zone and trough as parts of a discrete plate boundary dividing the Arabian and Indian plates.

The rates and azimuths determined from our model differ from those of prior models. For example, in our model at 18°N, 60.2°E, India is moving relative to Arabia at 2 mm/yr toward S22°W, parallel to the strike of the fracture zone. In contrast, prior models [*Chase*, 1978; *Minster and Jordan*, 1978] predict faster slip (10–14 mm/yr) that does not parallel the fracture zone; instead these models give directions of motion that are 35°–50° clockwise of the strike of the fracture zone, predicting a component of convergence of 7–8 mm/yr (Figure 7). Near the Dalrymple trough where seismic reflection profiles show listric normal faulting [*White*, 1984] and where focal mechanisms L, M, and N suggest active extension (Figure 1), the two earlier models predict a large component of convergence (Figure 7). Our model

TABLE 3. India-Arabia-Africa Euler Vectors From Three-Plate Model

Plate Pair	Latitude, °N	Longitude, °E	ω, deg m.y.$^{-1}$	Error Ellipse σ_{max}	σ_{min}	ζ_{max}	σ_ω, deg m.y.$^{-1}$
India-Arabia	3	92	0.03	26°	2°	N58°W	0.04
India-Africa	24	28	0.43	9°	2°	N73°W	0.06
Arabia-Africa	24	24	0.41	5°	1°	N64°W	0.05

The first plate moves counterclockwise relative to the second plate. One-sigma error ellipses are specified by the angular lengths of the principal axes and by the azimuths (ζ_{max}) of the major axis. Note that the rotation rate uncertainty is determined from a one-dimensional marginal distribution, whereas the lengths of the principal axes are determined from a two-dimensional marginal distribution.

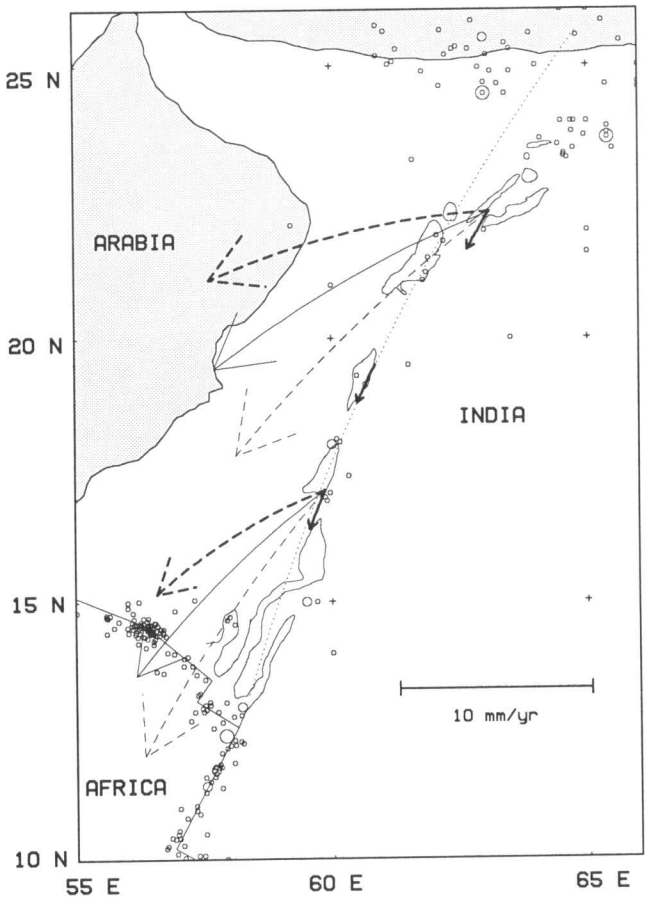

Fig. 7. Motion of India relative to Arabia along the Owen fracture zone and western Dalrymple trough. Plate motion models of *McKenzie and Sclater* [1971] (thin dashed curve), *Chase* [1978] (thin solid curve), *Minster and Jordan* [1978] (bold dashed curve), and the present study (bold solid curve) are compared. The new model indicates motion 4 to 8 times slower than prior models, in a significantly more southerly direction. A small circle (dotted curve) centered on our new India-Arabia Euler pole fits the Owen fracture zone north of 17°N well, but fits less well farther south. Where the northern end of the Owen fracture zone changes trend to meet the Dalrymple trough, the small circle fits badly, indicating extension in the Dalrymple trough, consistent with observations. Seismicity shown along the Owen fracture zone and Dalrymple trough includes events since 1910.

predicts mainly right-lateral strike slip with a small component of extension, as might be taken up along small pull-apart basins. Our prediction of a small component of extension across the Dalrymple trough is a direct consequence of assuming that pure right-lateral slip occurs across the northern Owen fracture zone.

Figure 5 also shows that prior plate motion models, including *Minster and Jordan's* [1978] model in which they divided the Indo-Australian plate into separate Australian and West-Indian plates, poorly fit the observed azimuths. That *Minster and Jordan's* [1978] model with separate Australian and West-Indian plates also disagrees with the observed azimuths shows that a good fit does not occur automatically if India and Australia are assumed to lie on separate plates. A necessary condition appears to be the exclusion from the India-Africa data set of spreading rates and transform azimuths along the Central Indian Ridge south of the equator.

The next step in our analysis was to place limits on the slip rate along the Owen fracture zone. A chi-square test gives an asymmetric 95% confidence interval of 0–7 mm/yr. Because a different chi-square test shows that we fit the data systematically better than expected, it is likely that we have overestimated the errors. Nevertheless, these conservative limits exclude the faster rates predicted by the models of *McKenzie and Sclater* [1971], *Chase* [1978], and *Minster and Jordan* [1978]. The formal lower bound differs only marginally from no motion along the Arabia-India boundary. However, the consistent sense of seismic slip along the Owen fracture zone, as well as documented recent extension in the Dalrymple trough, show that the motion is real, although possibly very slow.

Comparison To The Seismic Slip Rate

An independent estimate of the slip rate along the Arabia-India boundary can be obtained from its seismic moment release. Because of uncertainties in the moment-magnitude relationship, depth extent of faulting, and rigidity of the lithosphere, seismic slip rates are not highly accurate. Moreover, the interval over which the instrumental record extends may be too short to be representative of the long-term average moment release, and significant slip may be occurring aseismically. Nevertheless, the seismic slip rate can give an approximate lower bound on the slip rate and also can test our model because it potentially could show that motion was faster than the slow velocity we estimate here. We searched the earthquake data file of the NGDC and found 16 earthquakes along the Owen fracture zone that occurred between January 1963 and December 1985. Although the earthquakes are small (with body wave magnitudes ranging from 4.2 to 5.7), focal mechanisms along the boundary are consistent with local bathymetric trends and plate circuit closure, suggesting that these small earthquakes give useful information. For earthquakes with both m_b and M_s available, we used the latter. For earthquakes with only m_b available, we converted the body wave magnitudes to surface wave magnitudes using the scaling laws ($M_s = 3(m_b - 3.91)$ for $4.9 < M_s < 6.3$, and $M_s = 1.5(m_b - 2.28)$ for $2.9 < M_s < 4.9$) of *Geller* [1976]. We estimated seismic moments from surface wave magnitudes using the empirical scaling law ($\log M_0 = 1.08M_s + 19.1$) given by *Engeln et al.* [1986]. We obtained a total seismic moment release of 3.4×10^{25} dyn cm. We estimated the seismic slip rate from the following relation

$$\text{seismic slip rate} = \frac{\text{total seismic moment}}{(\text{fault area})(\text{rigidity})(\text{time window})} \quad (1)$$

[*Brune*, 1968]. We assumed a rigidity of 4×10^{11} dyn cm^{-2} [*Engeln et al.*, 1986], and assumed a depth of faulting of 15 km. Assuming that the fault includes the entire Owen fracture zone, which is about 1150 km long, we find a slip rate of 0.2 mm/yr. The slow seismic slip estimate may reflect a real slip rate of 0.2 mm/yr or it may grossly

underestimate the true slip. The slip rate is slower than, but within the confidence limits of, the 2 mm/yr rate of motion we estimated from the plate motion data. Although it shows that the slip rate is nonzero, the seismic moment release does not help to resolve the plate speed along the Owen fracture zone.

DISCUSSION

Because the motion along the Owen fracture zone is very slow, about 100 times slower than the fastest slipping transform along the East Pacific Rise, one might question whether the Owen fracture zone is a plate boundary. Realistically, motion along it is slow enough that it probably can be neglected in analysis of plate velocity circuits. Nevertheless, we think it is useful to model it as a plate boundary. First, it explains the modest difference in spreading rate on either side of the Owen transform fault. Second, it explains the alignment of seismicity starting near Karachi (Pakistan), extending southwestward through the Dalrymple trough, and continuing south-southwestward along and near the Owen fracture zone (Figure 1). Third, and most importantly, it explains the consistent direction of slip along the proposed Arabia-India plate boundary (Figure 5), including pure strike slip along the Owen fracture zone and a significant component of extension along Dalrymple trough. This pattern of slip seems distinctly different from regions of distributed intraplate seismicity, which do not exhibit consistent directions of slip although they may show consistent directions of principal strain axes. That azimuthal data extending over more than 1400 km are well fit by a single Euler pole supports a model in which the Owen fracture zone and Dalrymple trough compose a plate boundary along which slow motion occurs.

It is unclear how long the Owen fracture zone has played its current role in plate tectonics. Many workers have interpreted it to have been the locus of great left-lateral strike-slip faulting of India relative to Arabia-Africa before the rifting of the Gulf of Aden, but this has recently been disputed by *Mountain and Prell* [1987], who argue that the locus of faulting was farther west, along the Oman margin. Several workers have also suggested that the Murray ridge, and possibly the Owen ridge, record an earlier episode of contraction [e.g., *White*, 1984; *Mountain and Prell*, 1987], which must have preceded the current extension associated with the Dalrymple trough. In any event it seems unlikely that the current regime began before the rifting of the Gulf of Aden. We speculate that the Arabia-India boundary is now taking up slow motion caused by the contrast between subduction of Arabian oceanic lithosphere beneath Makran and the collisional resistance to further northward motion of India, a mechanism similar to that proposed by *Stein and Okal* [1978] to explain motion along the Ninetyeast Ridge. We also suggest that the plate boundary does not precisely follow the Owen fracture zone south of 17° because this southern segment is seismically quiet (Figures 1 and 7), and its trend does not parallel the direction of plate motion (Figure 5). Instead, the slip may be taken up in whole or in part along one or more north-northeast-striking lineaments west of the southern Owen fracture zone (Figure 1).

CONCLUSIONS

The Owen fracture zone is the locus of right-lateral strike-slip faulting. The best estimate of the slip rate is 2 mm/yr, with an upper bound of 7 mm/yr and a minimum slip rate of about 0.2 mm/yr. A significant component of normal faulting, presumably superimposed on right-lateral strike-slip faulting, occurs along the Dalrymple trough. Because the Owen fracture zone and Dalrymple trough compose a discrete line along which motion occurs in a consistent direction dividing aseismic regions, it seems reasonable to regard these features as the Arabian-Indian plate boundary, despite the slow rate of motion. This boundary may not follow the seismically quiet segment of the Owen fracture zone south of 17°N and may instead lie west of the southern Owen along or between one or more north-northeast striking linear ridges that join the Sheba Ridge.

Acknowledgments. We thank Emile Okal, Seth Stein, Dan McKenzie, and Bob White for helpful discussions, Paul Stoddard for use of his map-making program, Roger Searle for data in advance of publication, and Bernard Minster and an anonymous reviewer for helpful reviews. This research was supported by NSF grant EAR 8721306.

REFERENCES

Brune, J. N., Seismic moment, seismicity and rate of slip along major fault zones, *J. Geophys. Res., 73,* 777–784, 1968.

Chase, C. G., The N plate problem of plate tectonics, *Geophys. J. R. Astron. Soc., 29,* 117–122, 1972.

Chase, C. G., Plate kinematics: The Americas, East Africa, and the rest of the world, *Earth Planet. Sci. Lett., 37,* 355–368, 1978.

Cochran, J. R., The Gulf of Aden: Structure and evolution of a young ocean basin and continental margin, *J. Geophys. Res., 86,* 263–287, 1981.

Courtillot, V., A. Galdeano, and J. L. Le Mouel, Propagation of an accreting plate boundary: A discussion of new aeromagnetic data in the Gulf of Tadjurah and southern Afar, *Earth Planet. Sci. Lett., 47,* 144–160, 1980.

DeMets, C., R. G. Gordon, and D. F. Argus, Intraplate deformation and closure of the Australia-Antarctica-Africa plate circuit, *J. Geophys, Res., 93,* 11,877–11,897, 1988.

Dziewonski, A. M., and J. H. Woodhouse, An experiment in systematic study of global seismicity: Centroid-moment tensor solutions for 201 moderate and large earthquakes of 1981, *J. Geophys. Res., 88,* 3247–3271, 1983.

Dziewonski, A. M., J. E. Franzen, and J. H. Woodhouse, Centroid-moment tensor solutions for April–June 1983, *Phys. Earth Planet. Inter., 33,* 243–249, 1983.

Dziewonski, A. M., J. E. Franzen, and J. H. Woodhouse, Centroid-moment tensor solutions for July–September 1983, *Phys. Earth Planet. Inter., 34,* 1–8, 1984.

Dziewonski, A. M., J. E. Franzen, and J. H. Woodhouse, Centroid-moment tensor solutions for April–June 1985, *Phys. Earth Planet. Inter., 41,* 215–224, 1986*a*.

Dziewonski, A. M., J. E. Franzen, and J. H. Woodhouse, Centroid-moment tensor solutions for October–December 1985, *Phys. Earth Planet. Inter., 43,* 185–195, 1986*b*.

Dziewonski, A. M., G. Ekstrom, J. E. Franzen, and J. H. Woodhouse, Centroid-moment tensor solutions for July–September 1986, *Phys. Earth Planet. Inter., 46,* 305–315, 1987*a*.

Dziewonski, A. M., G. Ekstrom, J. E. Franzen, and J. H. Woodhouse, Global seismicity of 1977: centroid-moment tensor solutions for 471 earthquakes, *Phys. Earth Planet. Inter., 45,* 11–36, 1987*b*.

Dziewonski, A. M., G. Ekstrom, J. E. Franzen, and J. H. Woodhouse, Global seismicity of 1978: Centroid-moment tensor solutions for 512 earthquakes, *Phys. Earth Planet. Inter., 46,* 316–342, 1987*c*.

Engeln, J. F., D. A. Wiens, and S. Stein, Mechanisms and depths of Atlantic transform earthquakes, *J. Geophys. Res., 91,* 548–577, 1986.

Geller, R. J., Scaling relations for earthquake source parameters and magnitudes, *Bull. Seismol. Soc. Am., 66,* 1501-1523, 1976.

Girdler, R. W., C. Brown, D. J. M. Noy, and P. Styles, A geophysical survey of the westernmost Gulf of Aden, *Philos. Trans. R. Soc. London, Ser. A, 298,* 1–43, 1980.

Gordon, R. G., S. Stein, C. DeMets, and D. F. Argus, Statistical tests for closure of plate motion circuits, *Geophys. Res. Lett., 14,* 587–590, 1987.

Gutenberg, B., and C. F. Richter, *Seismicity of the Earth and Associated Phenomena* 2nd ed., Princeton University Press, Princeton, N.J., 1954.

Laughton, A. S., R. B. Whitmarsh, and M. T. Jones, The evolution of the Gulf of Aden, *Philos. Trans. R. Soc. London, Ser. A., 267,* 227–266, 1970.

Matthews, D. H., The Owen fracture zone and the northern end of the Carlsberg Ridge, *Philos. Trans. R. Soc. London, Ser. A, 259,* 172–186, 1966.

McKenzie, D. P., and J. G. Sclater, The evolution of the Indian Ocean since the late Cretaceous, *Geophys. J. R. Astron. Soc., 24,* 437–528, 1971.

Minster, J. B., and T. H. Jordan, Present-day plate motions, *J. Geophys. Res., 83,* 5331–5354, 1978.

Minster, J. B., T. H. Jordan, P. Molnar, and E. Haines, Numerical modeling of instantaneous plate tectonics, *Geophys. J. R. Astron. Soc., 36,* 541–576, 1974.

Mountain, G., and W. Prell, Leg 117 ODP Site Survey: A revised history of Owen Basin, *Eos Trans. AGU, 68,* 424, 1987.

Quittmeyer, R. C., and A. L. Kafka, Constraints on plate motions in southern Pakistan and the northern Arabian Sea from the focal mechanisms of small earthquakes, *J. Geophys. Res., 89,* 2444–2458, 1984.

Stein, S., and R. G. Gordon, Statistical tests of additional plate boundaries from plate motion inversions, *Earth Planet. Sci. Lett., 69,* 401–412, 1984.

Stein, S., and E. A. Okal, Seismicity and tectonics of the Ninetyeast Ridge area: Evidence for internal deformation of the Indian plate, *J. Geophys. Res., 83,* 2233-2245, 1978.

Sykes, L. R., Mechanism of earthquakes and nature of faulting on the mid-oceanic ridges, *J. Geophys. Res., 72,* 2131–2153, 1967.

Sykes, L. R., Seismological evidence for transform faults, seafloor spreading, and continental drift, in *The History of the Earth's Crust,* edited by R. A. Phinney, pp. 120–150, Princeton University Press, Princeton, N. J., 1968.

Sykes, L. R., Seismicity of the Indian Ocean and a possible nascent island arc between Ceylon and Australia, *J. Geophys. Res., 75,* 5041–5055, 1970.

Tamsett, D., and R. W. Girdler, Gulf of Aden axial magnetic anomaly and the Curie temperature isotherm, *Nature, 298,* 149–151, 1982.

Tamsett, D., and R. C. Searle, Structure and development of the mid-ocean ridge plate boundary in the Gulf of Aden: Evidence from GLORIA side scan sonar, *J. Geophys. Res., 93,* 3157-3178, 1988.

White, R. S., Active and passive plate boundaries around the Gulf of Oman,, *Deep Sea Res., Part A, 31 (6–8A),* 731–745, 1984.

Whitmarsh, R. B., The Owen Basin off the south-east margin of Arabia and the evolution of the Owen fracture zone, *Geophys. J. R. Astron. Soc., 58,* 441–470, 1979.

Wiens, D. A., C. DeMets, R. G. Gordon, S. Stein, D. Argus, J. F. Engeln, P. Lundgren, D. Quible, C. Stein, S. Weinstein, and D. F. Woods, A diffuse plate boundary model for Indian Ocean tectonics, *Geophys. Res. Lett., 12,* 429–432, 1985.

Wilson, J. T., A new class of faults and their bearing on continental drift, *Nature, 207,* 343–347, 1965.

C. DeMets, Naval Research Laboratory, Code 5110, Washington, DC 20375.

R. G. Gordon, Department of Geological Sciences, Northwestern University, Evanston, IL 60208.

(Received January 26, 1988;
revised September 12, 1988;
accepted October 13, 1988.)